

Analysis of the Localized Buckling in Composite Plate Structures with Application to Determining the Strength of Corrugated Fiberboard

REFERENCE: Johnson, M. W., Jr. and Urbanik, T. J., "Analysis of the Localized Buckling in Composite Plate Structures with Application to Determining the Strength of Corrugated Fiberboard," *Journal of Composites Technology & Research*, Vol. 11, No. 4, Winter 1989, pp. 121-127.

ABSTRACT: This study examines the theory for elastic buckling of composite structures composed of long rectangular flat plate elements. Elements can have nonlinear, orthotropic stress-strain properties characteristic of paper. Element stiffness coefficients add together to form a global structure stiffness matrix. Two methods of element counting and node labeling represent both determinant plate structures and periodic structures. Structure loading is in the axis direction of the plates. The solution gives the local buckling strain in the weakest structure element, which may differ from the weakest independent plate element. A nonlinear finite element method is developed with the finite elements being the plate elements of the structure. The small number of finite elements needed to characterize periodic structures makes the analysis efficient for searching out optimum designs. Corrugated fiberboard is one of the arbitrary structures appropriate for the analysis.

KEYWORDS: plate structures, elastic stability, buckling, corrugated fiberboard, paper, material failure, edgewise compression, component model, short column, nonlinear finite elements

Nomenclature

- A, B constants defined by Eq 17³
- $C = \frac{4(1 - \nu_1\nu_2)}{\nu_1 E_2} G$
- c_1, c_2 elastic coefficients
- E_1, E_2 orthotropic Young's moduli
- e strain invariant
- F dimensionless variable defined by Eq 22
- G shear modulus
- h plate thickness
- H plate strain energy density
- H_{ij} bending stiffness moduli
- $K_{aa}, K_{ab}, K_{ba}, K_{bb}$ element stiffness coefficients
- K_{ij} global stiffness coefficients
- ℓ plate half-width

- M_{ij} moment resultants
- m number of unique plates
- N_{ij} force resultants
- N_0 axial compressive force resultant
- NB global node label
- n number of unique nodes
- $[SK]$ global stiffness matrix
- S, W board dimensions (see Fig. 5)
- W_i board weight
- w transverse displacement component
- w'_a, w'_b nodal rotations
- x, y material Cartesian coordinates
- X, Y dimensionless variables defined by Eq. 22
- α, β root components of the characteristic equation (Eq 13)
- $\hat{\epsilon}, \hat{\epsilon}_1, \hat{\epsilon}_2, \hat{\epsilon}_r, \hat{\epsilon}_p, \hat{\epsilon}_s$ axial compressive strains
- $\epsilon_1, \epsilon_2, \epsilon_{12}$ middle surface strain components
- $\lambda, \lambda_1, \lambda_2, \lambda_r$ wave numbers
- ν_1, ν_2 orthotropic Poisson's ratios
- ρ plate density

Introduction

This paper examines the local instability of structural sections with flat plate elements under compression (Fig. 1). Historically, this subject was of interest to civil and aeronautical engineers and is discussed at some lengths by Bulson [1]. This existing

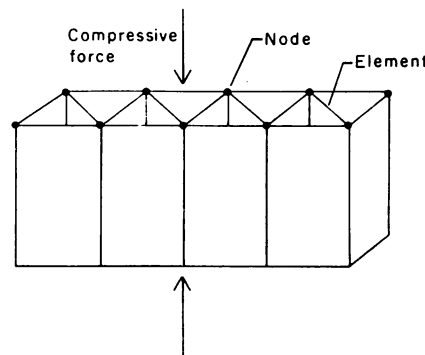


FIG. 1—Structural section with flat plate elements (ML88 5873).

¹Professor, Department of Engineering Mechanics, University of Wisconsin, 1415 Johnson Drive, Madison, WI 53706.

²Research general engineer, Forest Products Laboratory, 1 Gifford Pinchot Drive, Madison, WI 52705-2398.

theory is based on linear isotropic elasticity and is applicable to metal structures such as those encountered in aircraft design. We here extend the theory to account for elastic materials, such as paper, having nonlinear anisotropic properties.

In the section on basic elasticity equations we summarize the theory of plates of nonlinear orthotropic elastic material (developed previously [2]). In the section on element stiffness coefficients we use this theory to derive expressions for the stiffness coefficients of a single long plate element under uniaxial compression. In the following two sections we set forth the method and solution of a nonlinear finite element analysis that yields the critical buckling strain and load for structural sections of arbitrary configuration. Part of this analysis involves calculating the stiffness coefficients for each element using the results of the element stiffness coefficients section and assembling from them a global stiffness matrix.

This analysis has application to determine the strength of fiberboard under compression, which is one of the most important considerations in the design of fiberboard. In the section dealing with numerical results we present results for a fiberboard structure. The corrugating medium is approximated by flat plate elements as shown in Fig. 1.

The applications given here are only intended as illustrations of the use of the theory developed. Software based on this theory is being developed (by T. J. Urbanik) for use by packaging engineers. It is intended as easy-to-use software for the optimum design of corrugated containers.

Basic Elasticity Equations

The theory on which this paper is based was developed previously [2]. Equation (2.37)³ of that paper gives the equation of transverse force equilibrium in the form

$$\frac{\partial^2 M_{11}}{\partial x^2} + 2 \frac{\partial^2 M_{12}}{\partial x \partial y} + \frac{\partial^2 M_{22}}{\partial y^2} + \frac{\partial}{\partial x} \left(N_{11} \frac{\partial w}{\partial x} + N_{12} \frac{\partial w}{\partial y} \right) + \frac{\partial}{\partial y} \left(N_{22} \frac{\partial w}{\partial y} + N_{21} \frac{\partial w}{\partial x} \right) = 0 \quad (1)$$

where x and y are material Cartesian coordinates, M_{ij} moment resultants, N_{ij} force resultants, and w is the transverse displacement component.

In-plane stress-strain relations are given by Eqs (2.33) of Ref 2 as

$$\begin{aligned} N_{11} &= h \frac{\partial H}{\partial \epsilon_1} \\ N_{22} &= h \frac{\partial H}{\partial \epsilon_2} \\ N_{12} &= N_{21} = \frac{1}{2} h \frac{\partial H}{\partial \epsilon_{12}} \end{aligned} \quad (2)$$

where ϵ_1 , ϵ_2 , and ϵ_{12} are middle surface strain components, $H(\epsilon_1, \epsilon_2, \epsilon_{12})$ is the plate strain energy density function, and h the

³All equations with decimal notation represent expressions from the referenced sources.

plate thickness. Moment-curvature relations are given by Eqs (2.34) of Ref 2 as

$$\begin{aligned} M_{11} &= -\frac{1}{12} h^3 \left(H_{11} \frac{\partial^2 w}{\partial x^2} + H_{12} \frac{\partial^2 w}{\partial y^2} + H_{13} \frac{\partial^2 w}{\partial x \partial y} \right) \\ M_{22} &= -\frac{1}{12} h^3 \left(H_{12} \frac{\partial^2 w}{\partial x^2} + H_{22} \frac{\partial^2 w}{\partial y^2} + H_{23} \frac{\partial^2 w}{\partial x \partial y} \right) \\ M_{12} = M_{21} &= -\frac{1}{24} h^3 \left(H_{13} \frac{\partial^2 w}{\partial x^2} + H_{23} \frac{\partial^2 w}{\partial y^2} + H_{33} \frac{\partial^2 w}{\partial x \partial y} \right) \end{aligned} \quad (3)$$

The bending stiffness moduli H_{ij} are functions of the middle surface strains defined by

$$H_{11} = \frac{\partial^2 H}{\partial \epsilon_1^2}, \quad H_{12} = \frac{\partial^2 H}{\partial \epsilon_1 \partial \epsilon_2}, \dots$$

For some materials, including kraft paper, an adequate approximate theory [2] is obtained by taking H as a function of a single strain invariant

$$e = \epsilon_1^2/\nu_2 + \epsilon_2^2/\nu_1 + 2\epsilon_1\epsilon_2 + C\epsilon_{12}^2 \quad (4)$$

where

$$C = \frac{4(1 - \nu_1\nu_2)}{\nu_1 E_2} G$$

ν_1 and ν_2 are Poisson's ratios associated with extension in the 1 and 2 directions, respectively, G is the initial shear modulus, and E_2 the initial Young's modulus in the 2 direction. We call this an effective strain theory. For this theory, Eqs 2 give the in-plane stress-strain relations in the form

$$\begin{aligned} N_{11} &= 2hH'(e) (\epsilon_1/\nu_2 + \epsilon_2) \\ N_{22} &= 2hH'(e) (\epsilon_1 + \epsilon_2/\nu_1) \\ N_{12} = N_{21} &= hH'(e)C\epsilon_{12} \end{aligned} \quad (5)$$

and the bending stiffness moduli as

$$\begin{aligned} H_{11} &= 4H''(e) (\epsilon_1/\nu_2 + \epsilon_2)^2 + 2\nu_2^{-1}H'(e) \\ H_{22} &= 4H''(e) (\epsilon_1 + \epsilon_2/\nu_1)^2 + 2\nu_1^{-1}H'(e) \\ H_{12} &= 4H''(e) (\epsilon_1/\nu_2 + \epsilon_2) (\epsilon_1 + \epsilon_2/\nu_1) + 2H'(e) \\ H_{33} &= 4C^2H''(e)\epsilon_{12}^2 + 2CH'(e) \\ H_{13} &= 4CH''(e) (\epsilon_1/\nu_2 + \epsilon_2)\epsilon_{12} \\ H_{23} &= 4CH''(e) (\epsilon_1 + \epsilon_2/\nu_1)\epsilon_{12} \end{aligned} \quad (6)$$

Element Stiffness Coefficients

We assume that each plate element of the structure is in a homogeneous state of plane stress before buckling so that N_{ij} , ϵ_i , and H_{ij} are independent of x and y . Substituting Eqs 3 into

Eq 1, we obtain the following linear equation for w , the buckling perturbation

$$\begin{aligned} H_{11} \frac{\partial^4 w}{\partial x^4} + H_{22} \frac{\partial^4 w}{\partial y^4} + (2H_{12} + H_{33}) \frac{\partial^4 w}{\partial x^2 \partial y^2} \\ + 2H_{13} \frac{\partial^4 w}{\partial x^3 \partial y} + 2H_{23} \frac{\partial^4 w}{\partial x \partial y^3} \\ - \frac{12}{h^3} \left(N_{11} \frac{\partial^2 w}{\partial x^2} + 2N_{12} \frac{\partial^2 w}{\partial x \partial y} + N_{22} \frac{\partial^2 w}{\partial y^2} \right) = 0 \end{aligned} \quad (7)$$

We examine buckling modes of the form

$$w = e^{\lambda y + \alpha x} \quad (8)$$

Substituting Eq 8 into Eq 7 gives a fourth-degree equation for $\alpha(\lambda)$

$$\begin{aligned} H_{11} \alpha^4 + 2i\lambda H_{13} \alpha^3 - \left[(2H_{12} + H_{33}) \lambda^2 + \frac{12}{h^3} N_{11} \right] \alpha^2 \\ - \left(2\lambda^3 H_{23} + \frac{24}{h^3} N_{12} \lambda \right) i \alpha + H_{22} \lambda^4 + \frac{12}{h^3} N_{22} \lambda^2 = 0 \end{aligned} \quad (9)$$

Equation 9 holds for a material with general anisotropy and nonlinearity.

For a prebuckled state of uniaxial compression, we write

$$N_{22} = -N_0, \quad N_{11} = N_{12} = 0 \quad (10)$$

where N_0 is the axial compressive force resultant. We will also use the effective strain model. Equations 4 and 5 give $\epsilon_1 = -\nu_2 \epsilon_2$, $\epsilon_{12} = 0$, and

$$\begin{aligned} N_0 &= 2hH'(e)(1/\nu_1 - \nu_2)\hat{\epsilon} \\ e &= (1/\nu_1 - \nu_2)\hat{\epsilon}^2 \end{aligned} \quad (11)$$

where $\hat{\epsilon} = -\epsilon_2$ is the compressive strain. By Eqs 6, the stiffness moduli are

$$\begin{aligned} H_{11} &= 2\nu_2^{-1}H'(e) \\ H_{22} &= 4H''(\nu_2 - 1/\nu_2)^2\hat{\epsilon}^2 + 2\nu_1^{-1}H'(e) \\ H_{12} &= 2H'(e) \\ H_{33} &= 2CH'(e) \\ H_{13} &= H_{23} = 0 \end{aligned} \quad (12)$$

With Eqs 10 and 12, the characteristic Eq 9 becomes

$$H_{11} \alpha^4 - (2H_{12} + H_{33}) \lambda^2 \alpha^2 + H_{22} \lambda^4 - \frac{12}{h^3} \lambda^2 N_0 = 0 \quad (13)$$

Equation 13, being quadratic in α^2 , is readily solved. The four roots are denoted by α , $-\alpha$, $i\beta$, and $-i\beta$, where

$$\alpha = \left\{ \frac{2H_{12} + H_{33}}{2H_{11}} \lambda^2 + \left[\left(\frac{2H_{12} + H_{33}}{2H_{11}} \right)^2 \lambda^4 - \frac{H_{22}}{H_{11}} \lambda^4 + \left(\frac{N_0}{hH_{11}} \right) \frac{12\lambda^2}{h^2} \right]^{1/2} \right\}^{1/2} \quad (14)$$

$$\beta = \left(\alpha^2 - \frac{2H_{12} + H_{33}}{H_{11}} \lambda^2 \right)^{1/2}$$

We now assume that when buckling occurs, common edges of component plates remain straight. This has been observed [1] to be a good approximation for structural sections with flat plate elements. Hence, taking the edges at $x = \pm \ell$ (ℓ being plate half-width) and assuming both edges are in common with other plate elements, we impose the boundary conditions $w(\pm \ell) = 0$. Superposing the four solutions in the form of Eq 8 corresponding to the four roots of Eq 13 and satisfying $w(\pm \ell) = 0$ leads to the solution form

$$\begin{aligned} w = e^{\lambda y} [A(\cosh \alpha x \cos \beta \ell - \cosh \alpha \ell \cos \beta x) \\ + B(\sinh \alpha x \sin \beta \ell - \sinh \alpha \ell \sin \beta x)] \end{aligned} \quad (15)$$

where A and B are constants. The derivative of w is

$$\begin{aligned} \frac{\partial w}{\partial x} = e^{\lambda y} [A(\alpha \sinh \alpha x \cos \beta \ell + \beta \cosh \alpha \ell \sin \beta x) \\ + B(\alpha \cosh \alpha x \sin \beta \ell - \beta \sinh \alpha \ell \cos \beta x)] \end{aligned} \quad (16)$$

To establish local labels, denote the edges of the plate by subscripts a and b (Fig. 2). Setting $x = \pm \ell$ in Eq 16 yields

$$\begin{aligned} w'_a &= A(-\alpha \sinh \alpha \ell \cos \beta \ell - \beta \cosh \alpha \ell \sin \beta \ell) \\ &\quad + B(\alpha \cosh \alpha \ell \sin \beta \ell - \beta \sinh \alpha \ell \cos \beta \ell) \\ w'_b &= A(\alpha \sinh \alpha \ell \cos \beta \ell + \beta \cosh \alpha \ell \sin \beta \ell) \\ &\quad + B(\alpha \cosh \alpha \ell \sin \beta \ell - \beta \sinh \alpha \ell \cos \beta \ell) \end{aligned}$$

with w'_a and w'_b being defined by

$$\begin{aligned} w'_a &= e^{-\lambda y} \left. \frac{\partial w}{\partial x} \right|_a \\ w'_b &= e^{-\lambda y} \left. \frac{\partial w}{\partial x} \right|_b \end{aligned}$$

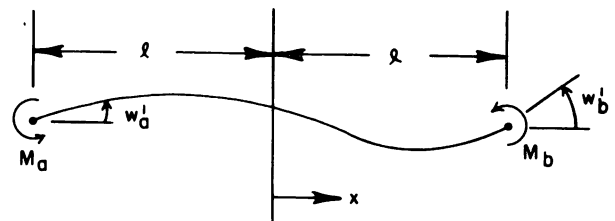


FIG. 2—Sign convention for positive edge moments and positive slopes through element cross section (ML88 5874).

Solving these two equations for A and B yields

$$A = \frac{w'_b - w'_a}{2(\alpha \sinh \alpha \ell \cos \beta \ell + \beta \cosh \alpha \ell \sin \beta \ell)} \quad (17)$$

$$B = \frac{w'_a + w'_b}{2(\alpha \cosh \alpha \ell \sin \beta \ell - \beta \sinh \alpha \ell \cos \beta \ell)}$$

The moment resultant M_{11} is given by Eqs 3. By Eqs 12, $H_{13} = 0$. Along an edge, $w = 0$ leads to $\partial^2 w / \partial y^2 = 0$, so that

$$x = \pm \ell: M_{11} = -\frac{1}{12} h^3 H_{11} \frac{\partial^2 w}{\partial x^2} \quad (18)$$

Define

$$M_a = e^{-i\lambda y} M_{11} \Big|_a$$

$$M_b = e^{-i\lambda y} M_{11} \Big|_b$$

and follow the sign convention for positively directed moments given in Fig. 2. Using Eqs 15, 17, and 18, we obtain the matrix formula

$$\begin{bmatrix} M_a \\ M_b \end{bmatrix} = \begin{bmatrix} K_{aa} & K_{ab} \\ K_{ba} & K_{bb} \end{bmatrix} \begin{bmatrix} w'_a \\ w'_b \end{bmatrix} \quad (19)$$

where the element stiffness coefficients are given by

$$\begin{bmatrix} K_{aa} \\ K_{ab} \end{bmatrix} = \frac{1}{24} h^3 H_{11} (\alpha^2 + \beta^2) \times \left(\pm \frac{1}{\alpha \tanh \alpha \ell + \beta \tan \beta \ell} + \frac{\tanh \alpha \ell \tan \beta \ell}{\alpha \tan \beta \ell - \beta \tanh \alpha \ell} \right) \quad (20)$$

$$K_{ba} = K_{ab}$$

$$K_{bb} = K_{aa}$$

From Eqs 14, note that

$$\alpha^2 + \beta^2 = \frac{1}{H_{11}} \times \left[(2H_{12} + H_{33})^2 \lambda^4 - 4H_{11} \left(\lambda^4 H_{22} - \frac{12}{h^3} N_0 \lambda^2 \right) \right]^{1/2} \quad (21)$$

Next, introduce dimensionless variables

$$F = \ell \beta, \quad X = \lambda \ell, \quad Y = \alpha \ell \quad (22)$$

The stiffness coefficients take the form

$$\begin{bmatrix} K_{aa} \\ K_{ab} \end{bmatrix} = \frac{1}{24} \frac{h^3}{\ell} H_{11} (Y^2 + F^2) \times \left(\pm \frac{1}{Y \tanh Y + F \tan F} + \frac{\tanh Y \tan F}{Y \tan F - F \tanh Y} \right) \quad (23)$$

From Eq 21

$$Y^2 + F^2 = \left[\left(\frac{2H_{12} + H_{33}}{H_{11}} \right)^2 X^4 - 4 \left(X^4 \frac{H_{22}}{H_{11}} - \frac{12\ell^2 X^2}{h^2} \frac{N_0}{hH_{11}} \right) \right]^{1/2} \quad (24)$$

From Eqs 14

$$Y^2 = \left(\frac{2H_{12} + H_{33}}{2H_{11}} \right) X^2 + \left[\left(\frac{2H_{12} + H_{33}}{2H_{11}} \right)^2 X^4 - \frac{H_{22}}{H_{11}} X^4 + \frac{12\ell^2 X^2}{h^2} \left(\frac{N_0}{hH_{11}} \right) \right]^{1/2} \quad (25)$$

$$F^2 = Y^2 - \frac{2H_{12} + H_{33}}{H_{11}} X^2 \quad (26)$$

Global Stiffness Matrix and Buckling Strain

When a structural section made of flat plate elements is compressed (Fig. 1), failure often initiates due to local buckling of the plate elements. This buckling defines the "short column" strength of the section. We develop here the formulas for a computer program to calculate the short column strength of sections of arbitrary topology.

We now assume that the wave numbers of the buckles, which occur in all plates simultaneously, are the same in each plate element $[I]$. This common wave number is denoted by λ . For triangular truss sections, critical buckling modes with inclined nodal lines in each plate element are possible [3–5]. The wave numbers are the same for each plate element, but a phase shift from one nodal line to adjacent lines occurs. Inclined nodal lines can be treated by superposing solutions of the form $w = e^{i(\lambda y + q) + \alpha x}$, where q is the phase shift, and modifying the analysis of the section on Element Stiffness Coefficients. We do not further consider inclined nodal lines in this paper.

The original angle between adjacent plates at their common edge is maintained during buckling $[I]$. Hence, the rotation of each plate joined at a node is taken to be the same. We code the structure with a set of plate labels 1, 2, . . . , m and node labels 1, 2, . . . , n , n being the rotational degrees of freedom. The sum of the moments applied to each node must be zero. Using Eq 19 to sum moments at each node yields a set of equations given in matrix form by

$$\begin{bmatrix} \Sigma M_1 \\ \Sigma M_2 \\ \vdots \\ \Sigma M_n \end{bmatrix} = \begin{bmatrix} K_{11} & K_{12} & \cdots & K_{1n} \\ K_{21} & K_{22} & \cdots & K_{2n} \\ \vdots & \vdots & \ddots & \vdots \\ K_{n1} & K_{n2} & \cdots & K_{nn} \end{bmatrix} \begin{bmatrix} w'_1 \\ w'_2 \\ \vdots \\ w'_n \end{bmatrix} = \begin{bmatrix} 0 \\ 0 \\ \vdots \\ 0 \end{bmatrix}$$

or

$$[\mathbf{SK}] [w'] = [0] \quad (27)$$

Stiffness coefficients K_{ij} of the global matrix $[\mathbf{SK}]$ are determined by assigning global node numbers to the local labels, forming the stiffness matrix (Eq 19) for each element, and summing the coefficients according to

$$K_{ij} = \sum_{L=1}^m \sum_a \sum_b K_{ab}^L \quad (28)$$

where K_{ab}^L is the contribution to global stiffness coefficient K_{ij} of local element K_{ab} of plate element L .

Periodic structures are analyzed by examining a repeating group of plates. The degrees of freedom are reduced to the set of nodes interior to a repeating group by using the fact that the rotation at a node exterior to the group is the negative of the rotation of one of the interior nodes. We code exterior nodes with labels from the set 1, 2, . . . , n . The local element coefficients added to the global matrix are taken from the row matrix

$$\begin{aligned} a > 0, b < 0: & \quad [K_{aa} \quad -K_{a(-b)}] \\ a < 0, b > 0: & \quad [-K_{(-a)b} \quad K_{bb}] \end{aligned}$$

Using Eqs 11, 14, and 20, we see that the elements of matrix $[\mathbf{SK}]$ are functions of the axial strain $\hat{\epsilon}$ applied to the structure and of the wave number λ . The critical strains are those values for which stiffness matrix $[\mathbf{SK}]$ is singular, allowing Eq 27 to have a nontrivial solution for the rotation vector. These critical strains are hence solutions of the equation

$$f(\hat{\epsilon}, \lambda) \equiv \det [\mathbf{SK}] = 0 \quad (29)$$

For a single plate with simply supported edges, the critical buckling strain is determined from the equation $\tan F = \infty$, while for a plate with fixed edges it is determined from $Y \tanh Y + F \tan F = 0$ [6]. Therefore, we can see from the form of the stiffness coefficients (Eq 23) that infinities of function $f(\hat{\epsilon}, \lambda)$ will occur at the fixed-edge buckling strain of each plate element. At values of $\hat{\epsilon}$ near buckling, function $f(\hat{\epsilon}, \lambda)$ has the form shown in Fig. 5 of Ref 6 where an optimum λ exists that yields a minimum $\hat{\epsilon}$. At nonoptimum fixed values for λ , this function takes one of the forms shown in Fig. 3, with the first singularity being at $\hat{\epsilon}_p$, the lowest of critical strains at the nonoptimum wavelength for elements with fixed edges. Simple zeros occur as illustrated in Fig. 3a. Figure 3b illustrates three other possibilities that occur. The optimal λ in these latter cases corresponds to a zero of higher order (zero at a relative minimum).

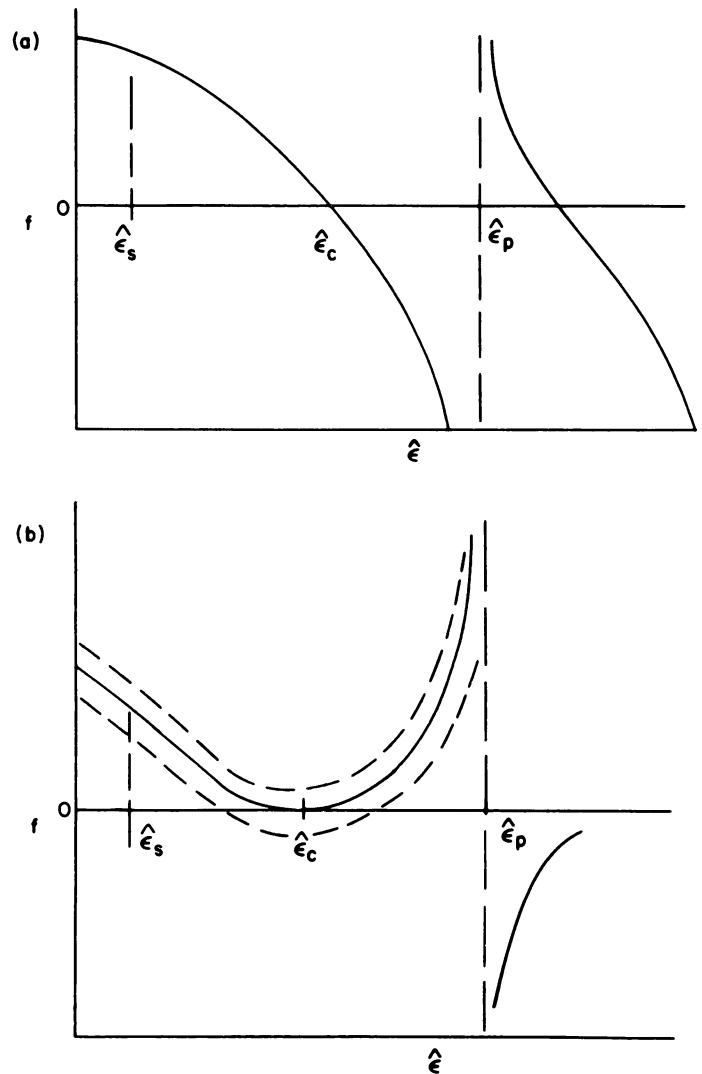


FIG. 3—Form of function $f(\hat{\epsilon}, \lambda)$. Solution algorithm: (a) Modified regular falsi; (b) golden section. (ML88 5869)

Algorithm for Finding Minimum $\hat{\epsilon}$

Our program for calculating the buckling strain of a plate structure first calculates the buckling strains of each plate having either a simply supported or fixed-edge condition, a problem solved previously [6]. The buckling strains and wave numbers found there are used to guide the solution for the structure.

The solution of Eq 29 yields a root $\hat{\epsilon}$ for fixed λ . Initially, roots $\hat{\epsilon}_1$ and $\hat{\epsilon}_2$ are found for wave numbers λ_1 and λ_2 . Wave number λ_1 corresponds to the lowest simple support wave number of the set of plate elements and λ_2 to the wave number of the weakest plate element with fixed-edge conditions. An updated estimate of the optimum value λ_r , yielding the minimum root $\hat{\epsilon}$, is calculated from

$$\lambda_r = \sqrt{\frac{\sqrt{\hat{\epsilon}_2} \lambda_1 - \sqrt{\hat{\epsilon}_1} \lambda_2}{\sqrt{\hat{\epsilon}_1} \lambda_2 - \sqrt{\hat{\epsilon}_2} \lambda_1}} \quad (30)$$

This formula is obtained by first determining a and b in the form $\sqrt{\hat{\epsilon}} = a/\lambda + b/\lambda$ by evaluating this expression at λ_1 and λ_2 . The value of λ that minimizes this form is given by $\sqrt{a/b}$, from which Eq 30 is obtained.

The iterations proceed as follows:

1. Using λ_c , determine a root $\hat{\epsilon}_c$ from Eq 29.
2. Assign new values of λ_1 and λ_2 from the present λ_1 , λ_2 , and λ_c by choosing the two values that correspond to the two smallest roots of Eq 29.
3. Update λ_c with Eq 30.
4. Go to 1. Continue iteration until convergence of λ_c is indicated.

The subprogram for calculating a root $\hat{\epsilon}$ of Eq 29 utilizes the fact that for any λ , $\hat{\epsilon}$ is bounded by two values. A lower bound, $\hat{\epsilon}_s$, equals the critical value for the weakest plate with simply supported edges. An upper bound, at $\hat{\epsilon}_p$, equals the lowest singularity of Eq 29. This is illustrated in Fig. 3. The function may have a simple zero, in which case a modified regula falsi method [7] is used, or it may have a relative minimum that approximates the root, in which case the golden section algorithm is used.

The subprogram for calculating $\hat{\epsilon}_p$ finds the singularity at λ for each plate by first solving Eq (4.4) of Ref 6 using fixed-point iteration and then using either fixed-point or Newton's iteration to solve Eqs (2.12) and (2.13) of Ref 6. Then $\hat{\epsilon}_p$ is the lowest singularity. The plate having the lowest singularity is the one that initiates structure buckling. A final subprogram assembles the global matrix **[SK]** and computes its determinant.

Program running time is sensitive to the relative error criteria for testing convergence. We found, however, that the errors used to calculate $\hat{\epsilon}_p$ and λ_c are much less critical than the error used to calculate a root $\hat{\epsilon}$. We further reduce running time by retaining values from each iteration to initialize succeeding iterations.

Our algorithm has successfully determined the strength of a large number of diverse singlewall and multiwall corrugated fiberboard and box-type structures. Of course, structures may yet be found that defy our algorithm. For these cases, an exhaustive search patterned after Fig. 5 of Ref 6 can determine the critical strain by examining determinant values calculated from Eq 29 over an array of $\hat{\epsilon}$ and λ combinations.

Numerical Results for Fiberboard Structures

In an earlier publication [2] we developed a mathematical model for the elastic behavior of paper that incorporates non-linearity and anisotropy. For uniaxial compression of paper in the y direction (across machine direction), the expression

$$-N_{22} = N_0 = hc_1 \tanh(c_2 \hat{\epsilon}/c_1) \quad (31)$$

fits the data for kraft paper well. Here, c_1 and c_2 are constants, and $\hat{\epsilon}$ is the axial compressive strain. An effective strain theory is used in Ref 2 with the function H' determined from Eqs 11 and 31 in the form

$$H'(e) = \frac{c_1}{2\sqrt{(1/\nu_1 - \nu_2)e}} \tanh\left(\frac{c_2}{c_1} \sqrt{\frac{e}{1/\nu_1 - \nu_2}}\right)$$

Using this relation and Eqs 12, we obtain the following expressions for the bending stiffness moduli

$$\begin{aligned} H_{11} &= \frac{c_1 \nu_1 / \nu_2}{1 - \nu_1 \nu_2} \frac{\tanh(c_2 \hat{\epsilon} / c_1)}{\hat{\epsilon}} \\ H_{22} &= \frac{c_2}{\cosh^2(c_2 \hat{\epsilon} / c_1)} + \frac{\nu_1 \nu_2 c_1}{1 - \nu_1 \nu_2} \frac{\tanh(c_2 \hat{\epsilon} / c_1)}{\hat{\epsilon}} \\ H_{12} &= \frac{c_1 \nu_1}{1 - \nu_1 \nu_2} \frac{\tanh(c_2 \hat{\epsilon} / c_1)}{\hat{\epsilon}} \\ H_{33} &= \frac{4(1 - \nu_1 \nu_2)G}{\nu_1 E_2} H_{12} \\ H_{13} &= H_{23} = 0 \end{aligned} \quad (32)$$

We use the following approximation [2] because of St. Venant [8]

$$G = \frac{\sqrt{E_1 E_2}}{2(1 + \sqrt{\nu_1 \nu_2})} \quad (33)$$

where E_1 is the initial Young's modulus in the x direction. We next derive

$$\begin{aligned} \frac{2H_{12} + H_{33}}{2H_{11}} &= \sqrt{\nu_2 / \nu_1} \\ \frac{H_{22}}{H_{11}} &= \nu_2^2 + \frac{\nu_2}{\nu_1} (1 - \nu_1 \nu_2) \frac{2c_2 \hat{\epsilon} / c_1}{\sinh(2c_2 \hat{\epsilon} / c_1)} \\ \frac{N_0}{hH_{11}} &= \frac{\nu_2}{\nu_1} (1 - \nu_1 \nu_2) \hat{\epsilon} \end{aligned} \quad (34)$$

Expressions from Eqs 34 are used in Eqs 23 to 26 for calculating the element stiffness coefficients.

In our program for calculating critical buckling loads of fiberboard structural sections, the input is composed of the element label, node labels, dimensions, and stress-strain parameters characterizing each plate element. A counting pattern establishes the unit structure length in terms of the replicated elements. Further notational detail appears in Table 1.

The $m \times 2$ connection matrix with element **NB**(I, J) describes how the plate elements are connected to form a structure. Index I labels the plate element, index J labels the plate node; J ($= 1, 2$) is a local node label. The absolute value of **NB** is the global label of the node with local label (I, J). Element NB is positive if the node is a node interior to a repeating group, and it is negative if the node is related to an interior node by a periodicity requirement. The requirement used here is that the rotation of the node should be of the same magnitude as but opposite in sign to the periodically related node.

The program output includes the critical strain of the structure, the associated wave number λ , and the critical force per board element length. Calculated results for a periodic truss core structure representing C-flute corrugated fiberboard are shown in Fig. 4.

This example shows how structure elements can mutually stabilize each other. Element 5, representing the core, has a lower buckling strain than does a facing element under simple support or fixed-edge conditions. However, in the structure, Element 1 yields the lowest singularity and therefore initiates buckling. We see from the output that the facing restrains the core edge ro-

TABLE 1—Printout headings.

Name	Description	Comments
L-Node	global node label of local node 1	
R-Node	global node label of local node 2	
Count	absolute value equals multiples of plate in board element	Board element length equals $\Sigma \ell$: Count < 0
t	element thickness (t) ^a	
ℓ	element width (ℓ)	
c1, c2	coefficients in stress-strain relation (f/ℓ^2) ^a	Eq 4.3 of Ref 2
A	ratio of c_2 (x direction) to c_2 (y direction)	Eq 4.8 of Ref 2
Nu	geometric mean Poisson's ratio	Ref 1
G	initial shear modulus (f/ℓ)	
S	dimensionless stiffness	Eq (2.10) of Ref 6 $K_{ax}; \dot{\epsilon} = 0$
D	initial x-direction bending stiffness coefficient (f)	
Ep	normalized strain	Eq 2.10 of Ref 6
Chi	dimensionless wave number	Eq 2.10 of Ref 6
Ratio 1	strain normalizing factor	$(c_2/c_1)/(c_2/c_1)_w$: w being weakest plate
Ratio 2	wave number normalizing factor	$(\ell/A^{1/4})/(\ell/A^{1/4})_w$
Ratio 3	stiffness normalizing factor	D/D_w
Sigma	dimensionless buckling stress	Eq 5.1 of Ref 6
Pct Load	load distribution among plates	Count $\neq 0$

^aUnits: 1 denotes length in inches (mm), f denotes force in pounds (newtons).

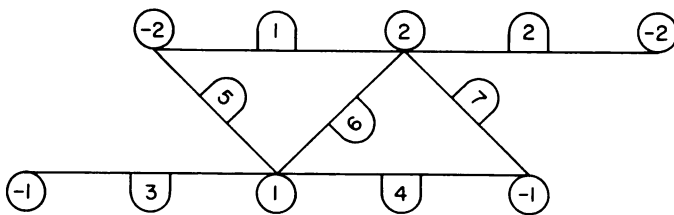


FIG. 4—C-flute structure for program output shown on right. (ML88 5872)

tation much more than the core restrains the facings. Therefore, under these conditions of mutual restraint, the facings buckle first.

Concluding Remarks

We have developed an algorithm for computing the strength of plate structures of arbitrary configuration and show results for a structure modeling C-flute corrugated fiberboard. We have applied the algorithm successfully to a wide variety of corrugated and box-type structures.

Our main interest in developing this program is for application to optimal design of corrugated fiberboard structures. For example, the structure can be optimized following the methodology set forth in Ref 9 and using the weakest element determined by this program.

Figures 5 and 6 illustrate the use of the program to optimize the design of a structure. The configuration of the structure is

Plate Number	Repliated Plate	Global L Node	Global R Node	Count per Period	Thickness t	Width 1
1	1	-2	2	1.00	.01200	.3077
2	1	2	-2	.00	.01200	.3077
3	1	-1	1	1.00	.01200	.3077
4	1	1	-1	-1.00	.01200	.3077
5	5	-2	1	1.00	.00800	.2277
6	5	1	2	1.00	.00800	.2277
7	5	2	-1	.00	.00800	.2277

	Stress-Strain Parameters				Stiffness S	Stiffness D
	c1	c2	A	Nu	G/c2	
1	1800.	340000.	2.5000	.2680	.6235	.4542
2	1800.	340000.	2.5000	.2680	.6235	.4542
3	1800.	340000.	2.5000	.2680	.6235	.4542
4	1800.	340000.	2.5000	.2680	.6235	.4542
5	1000.	125000.	2.2000	.2680	.5849	.2289
6	1000.	125000.	2.2000	.2680	.5849	.2289
7	1000.	125000.	2.2000	.2680	.5849	.2289

	Normalized Buckling Parameters				Buckling Parameters			
	Simple Ep	Fixed Ep	Simple Chi	Fixed Chi	Simple Strain	Fixed Strain	Simple Wave Number	Fixed Wave Number
1	1.327	1.858	1.951	3.432	.007025	.009836	15.95	28.05
2	1.327	1.858	1.951	3.432	.007025	.009836	15.95	28.05
3	1.327	1.858	1.951	3.432	.007025	.009836	15.95	28.05
4	1.327	1.858	1.951	3.432	.007025	.009836	15.95	28.05
5	.751	1.145	1.702	2.827	.006008	.009161	18.21	30.24
6	.751	1.145	1.702	2.827	.006008	.009161	18.21	30.24
7	.751	1.145	1.702	2.827	.006008	.009161	18.21	30.24

Weakest independent plate: 5
Weakest system plate : 1

System buckling strain = .7178E-02
System wave number = 16.97
System strength = 46.28

Plate	System buckling parameters				Ratio 1	Ratio 2	Ratio 3
	Ep	Chi	Sigma	Pct. Load			
1	1.356	2.076	.875	40.86	1.511	1.309	7.720
2	1.356	2.076	.875	.00	1.511	1.309	7.720
3	1.356	2.076	.875	.00	1.511	1.309	7.720
4	1.356	2.076	.875	40.86	1.511	1.309	7.720
5	.897	1.586	.715	9.14	1.000	1.000	1.000
6	.897	1.586	.715	9.14	1.000	1.000	1.000
7	.897	1.586	.715	.00	1.000	1.000	1.000

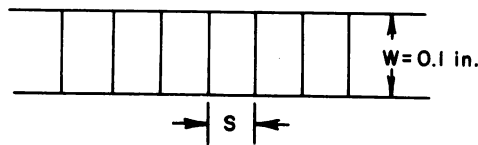
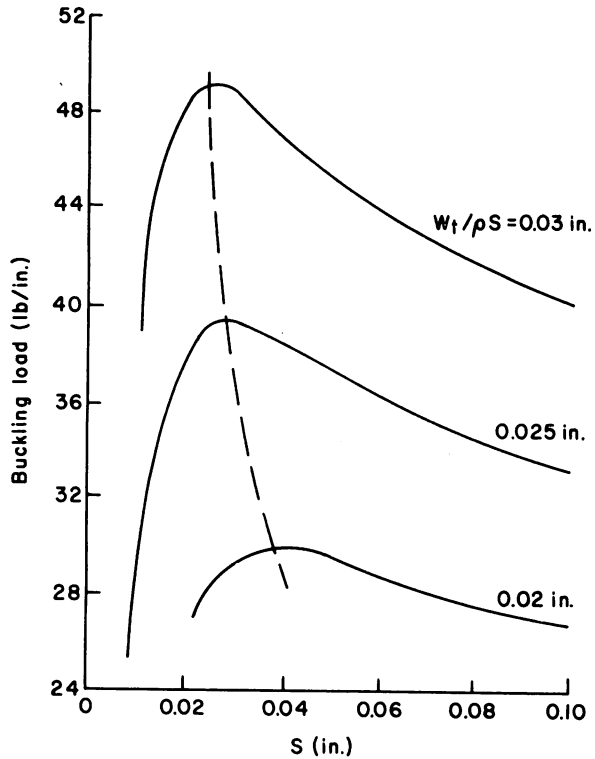


FIG. 5—Buckling load as a function of spacing S . (ML88 5871)

shown in Fig. 5. Each plate element has Poisson's ratios $\nu_1 = 0.36$, $\nu_2 = 0.2$, and $c_1 = 2000$ psi, $c_2 = 0.4 \times 10^6$ psi. The weight of a board element is given by

$$W_i = \rho(2Sh + Wh) \tag{35}$$

where ρ is the plate density, dimensions S and W are shown on Fig. 5, and h is the plate element thickness. Solving Eq 35 we obtain an equation for h as a function of S

$$h(S) = \frac{W_i/\rho S}{2 + W/S} \tag{36}$$

We wish to choose spacing S that minimizes the board weight W_i/S for a given strength. Dimension W is fixed at $W = 0.1$ in. For constant $W_i/\rho S$, h is determined from Eq 36 as a function of S , and the program is used to determine the buckling load. Figure 5 shows the buckling load as a function of S for constant W_i/S . The maxima of the curves give the optimal values of S

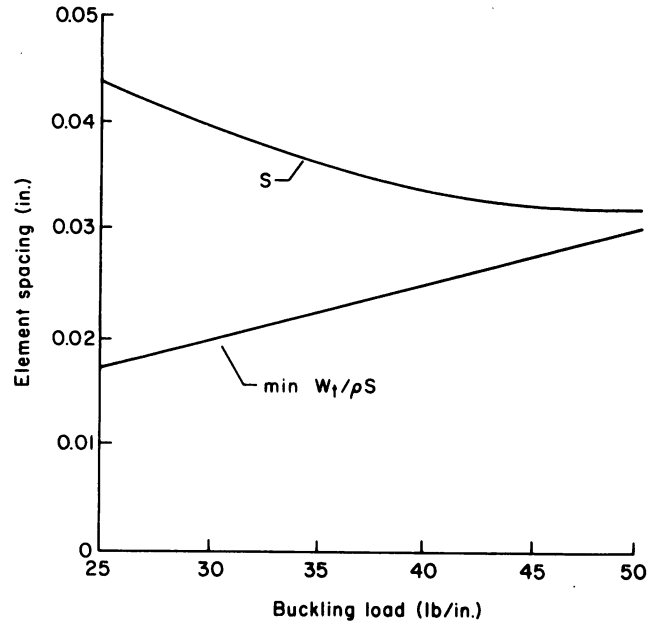


FIG. 6—Optimal value of board weight and S . (ML88 5870)

that minimize the board weight for a given buckling load. Optimal values of S and the associated minimum board weights are replotted in Fig. 6.

Acknowledgment

The Forest Products Laboratory is maintained in cooperation with the University of Wisconsin. This article was written and prepared by U.S. Government employees on official time, and it is therefore in the public domain and not subject to copyright.

References

- [1] Bulson, P. S., *The Stability of Flat Plates*, American Elsevier, New York, 1969, p. 295.
- [2] Johnson, M. W. and Urbanik, T. J., *Journal of Applied Mechanics*, Vol. 51, Mar. 1984, pp. 146-152.
- [3] Zahn, J. J., "Local Buckling of Orthotropic Truss-Core Sandwich," USDA Forest Service, Forest Products Laboratory, Research Paper FPL 220, 1973.
- [4] Wittrick, W. H. and Curzon, P. L. V., *Aeronautics Quarterly*, Vol. 20, 1969, pp. 122.
- [5] Wittrick, W. H., *International Journal of Mechanical Sciences*, Vol. 14, 1972, pp. 263-271.
- [6] Johnson, M. W. and Urbanik, T. J., *Wood and Fiber Science*, Vol. 19, Apr. 1987, pp. 135-146.
- [7] Rice, J. R., *Numerical Methods, Software, and Analysis* (IMSL Reference Edition), McGraw Hill, New York, 1983, pp. 222-225.
- [8] Lekhnitskii, S. G., *Theory of Elasticity of an Anisotropic Elastic Body*, Holden-Day, San Francisco, 1963, p. 55.
- [9] Urbanik, T. J., "Effect of Paperboard Stress-Strain Characteristics on Strength of Singlewall Corrugated Fiberboard: A Theoretical Approach," USDA Forest Service, Forest Products Laboratory, Research Paper FPL 401, 1981.